Photoreflectance study of narrow-well strained-layer $In_xGa_{1-x}As/GaAs$ coupled multiple-quantum-well structures

S. H. Pan,* H. Shen, Z. Hang,† and F. H. Pollak†
Physics Department, Brooklyn College of the City University of New York, Brooklyn, New York 11210

Weihua Zhuang and Qian Xu
Institute of Semiconductors, Chinese Academy of Sciences, P.O. Box 912, Beijing, China

A. P. Roth, R. A. Masut, C. Lacelle, and D. Morris
Division of Physics, National Research Council of Canada, Ottawa, Canada K1A 0R6
(Received 5 February 1988)

We have measured the photoreflectance (PR) spectra at 300 and 77 K of two strained-layer [001] $In_xGa_{1-x}As/GaAs$ ($x \approx 0.12$) multiple quantum wells (MQW's) with nominal well (L_Z) and barrier (L_B) widths of (50 Å)/(100 Å) and (30 Å)/(100 Å), respectively, as deduced from the growth conditions. In both samples we have observed a number of features in the PR spectra corresponding to miniband dispersion (coupling between wells) of both confined and unconfined (above the GaAs barrier) transitions. The coupling between wells leads to different transition energies at the mini-Brillouin-zone center (Γ) and the edge (π) along the growth direction. This is the first observation of unconfined features and miniband dispersion in this system. Even though our samples have fairly wide barriers ($L_B \approx 100$ Å), the coupling between wells is an important effect because of the relatively small confinement energies for $x \approx 0.12$. Using the envelope-function approach, we have calculated the various transition energies taking into account both strain and quantum-well effects, including miniband dispersion. Good agreement with experiment is found for a heavy-hole valence-band discontinuity of 0.3 ± 0.05 and $L_Z/L_B = (52 \pm 3$ Å$)/(105 \pm 5$ Å$)$ ($x = 0.11 \pm 0.01$) and $(32 \pm 3$ Å$)/(95 \pm 5$ Å$)$ ($x = 0.12 \pm 0.01$) for the two samples, respectively. The In composition and well and barrier widths are thus in good agreement with the growth conditions. Although the symmetric component of the fundamental light-hole–to–conduction-subband transition is a strong feature, the small observed amplitude of the antisymmetric component for both samples is evidence for the type-II nature of the light-hole–to–conduction-subband transitions.

I. INTRODUCTION

During the past several years there has been considerable interest in the strained-layer $In_{1-x}Ga_xAs/GaAs$ system from both fundamental and applied points of view.[1–8] Strained-layer heterostructures allow the use of lattice-mismatched materials without the generation of misfit dislocations. This freedom from the need for precise lattice matching widens the choice of compatible materials and greatly increases the ability to control the electronic and optical properties of such structures. One of the most important fundamental questions about this system is the nature of the band offset. Marzin, Charasse, and Sermage reported optical-absorption studies of multiple quantum wells (MQW's) with $x \approx 0.15$.[1] They explained their observations using a heavy-hole valence-band offset (Q_V^{HH}) of about 0.3. The valence- and conduction-band offsets Q_V and Q_C are defined as $Q_V = \Delta E_V/(\Delta E_V + \Delta E_C)$ and $Q_C = 1 - Q_V$, where ΔE_V and ΔE_C are the valence- and conduction-band discontinuities at the heterojunction. Such an alignment would lead to the interesting result that the heavy holes are confined in the $In_xGa_{1-x}As$ layers (type-I superlattice) while the light holes are confined in the GaAs region (type-II superlattice). The work of Reddy *et al.*[4] and Ji *et al.*[5–7] using various optical methods such as transmission and photoreflectance are in agreement with the conclusion of Marzin, Charasse, and Sermage. However, a recent study of Menendez *et al.*[8] using a light-scattering method and photoluminescence excitation spectroscopy contradicts previous experimental results. In their band-alignment scheme, both heavy and light holes are confined in the $In_xGa_{1-x}As$ layers.

In order to gain more information about this interesting system we have studied the photoreflectance (PR) spectra at 300 and 77 K of two [001] $In_xGa_{1-x}As/GaAs$ ($x \approx 0.12$) MQW's. Our samples have nominal well (L_Z) and barrier (L_B) widths of (50 Å)/(100 Å) and (30 Å)/(100 Å). There is significant coupling between wells even for the fundamental heavy-hole–to–conduction-subband transition. This interaction is due to a combination of relatively small confinement energies and barrier widths in our materials. This coupling leads to different transition energies at the mini-Brillouin-zone center (Γ) and edge (π) along the growth direction (miniband dispersion). We have observed a number of PR features at both temperatures including symmetry-allowed and -forbidden transitions, confined and above-barrier

 ©1988 The American Physical Society

(unconfined) features, and the influence of the coupling. The origins of the various spectral features have been identified by comparison with a theoretical calculation based on the envelope-function model.[9] We find a value of $Q_V^{HH}=0.3\pm0.05$ for both samples. In addition, evidence for the type-II nature of the light-hole transition is deduced from observations related to the symmetry properties of miniband dispersion transitions in such a superlattice. This experiment is the first report of coupling effects and above-barrier transitions in this system. The formation of miniband dispersion is an additional degree of freedom which is of great value in the interpretation of our results.

II. EXPERIMENTAL DETAILS

In $In_xGa_{1-x}As$/GaAs MQW samples used in our study were grown by metal-organic vapor-phase epitaxy on [001] GaAs substrates.[10] A 600-Å GaAs buffer was grown on the substrate before the MQW fabrication. The nominal L_Z and L_B are (50 Å)/(100 Å) (sample A) and (30 Å)/(100 Å) (sample B). Sample A is lightly doped with Mg ($p\sim10^{16}$ cm^{-3}) while sample B is undoped. From the growth conditions the In concentration is $x\approx0.12$. The PR apparatus has been described in the literature.[11] A 1-mW HeNe laser was used as the pump beam.

III. THEORETICAL BACKGROUND

When grown on a GaAs buffer the $In_xGa_{1-x}As$ layers substain a biaxial in-plane compression and a corresponding extension along the [001] growth direction. In general, since the GaAs buffer layer is much thicker than the $In_xGa_{1-x}As$ layers the biaxial strain ε is given by

$$\varepsilon=(a_{l,2}-a_{l,1})/a_{l,1}\ , \tag{1}$$

where $a_{l,1}$ and $a_{l,2}$ are the lattice constants of the $In_xGa_{1-x}As$ and GaAs, respectively. The former is obtained by a linear interpolation between the lattice constants of InAs and GaAs.

This strain alters the band structure of the $In_xGa_{1-x}As$/GaAs MQW. The strain-dependence conduction (C) to heavy- (HH) and light- (LH) hole energy gaps is thus[12]

$$E_0^{C,HH}=E_0(In_xGa_{1-x}As)+\delta E_H-\delta E_S\ , \tag{2a}$$

$$E_0^{C,LH}=E_0(In_xGa_{1-x}As)+\delta E_H+\delta E_S-(\delta E_S)^2/2\Delta_0+\cdots\ . \tag{2b}$$

In Eqs. (2), $E_0(In_xGa_{1-x}As)$ is the unstrained direct band gap of the $In_xGa_{1-x}As$ and Δ_0 is the spin-orbit splitting. The quantities δE_H (hydrostatic-pressure shift) and δE_S (uniaxial stress-induced valence-band splitting) are given by[12]

$$\delta E_H=2a[(C_{11}-C_{12})/C_{11}]\varepsilon\ , \tag{3a}$$

$$\delta E_S=b[(C_{11}+2C_{12})/C_{11}]\varepsilon\ . \tag{3b}$$

The parameters a and b are the interband hydrostatic pressure and uniaxial deformation potentials, respectively, and the C_{ij} are elastic-stiffness constants. The light-hole valence band has a nonlinear strain dependence because of the strain-induced coupling with the spin-orbit-split band.[12]

Since for our case $\varepsilon<0$ the effect of the lattice-mismatch strain is to (1) increase the energy gap of the $In_xGa_{1-x}As$ (hydrostatic-pressure component), and (2) split the degeneracy of the valence-band edge at the center of the Brillouin zone so that the heavy-hole band moves up and the light-hole band moves down, relative to the unstressed valence band. Thus, in such a system the relative positions of the bands in the $In_xGa_{1-x}As$ wells and the GaAs barriers can lead to two possible configurations of the superlattice potential as shown in Fig. 1. In the configuration on the left-hand side the electrons and both the heavy and light holes are confined in the $In_xGa_{1-x}As$ wells (type-I superlattice). However, in the configuration on the right-hand side the electrons and heavy holes are in the $In_xGa_{1-x}As$ region (type I) while the light holes are confined in the GaAs layers (type II).

The subband energies of the MQW structures were calculated using the envelope-function model[9] and the strain-induced shifts and splittings given above. The values of the various strain-related parameters used in the calculation are listed in Table I. A linear interpolation was used for the $In_xGa_{1-x}As$ values. The energy gaps and masses employed are given as follows:

$$E_0(In_xGa_{1-x}As)=E_0(GaAs)-1.53x+0.45x^2 \tag{4a}$$

at 300 K from Ref. 13,

$$E_0(In_xGa_{1-x}As)=E_0(GaAs)-1.47x+0.375x^2 \tag{4b}$$

at 77 K from Ref. 14,

$$\Delta_0=0.341-0.09x+0.14x^2 \tag{4c}$$

from Ref. 15,

$$m_C^*=(0.0665-0.044x)m_0 \tag{5a}$$

from Ref. 16,

$$m_{LH}^*=(0.094-0.062x)m_0 \tag{5b}$$

from Ref. 16, and

$$m_{HH}^*=(0.45-0.07)m_0 \tag{5c}$$

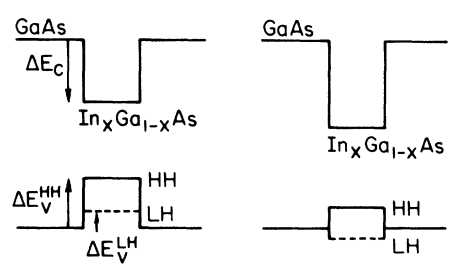

FIG. 1. Possible energy-band configurations in a strained-layer $In_xGa_{1-x}As$/GaAs quantum well. In the $In_xGa_{1-x}As$ layers the top of the valence band is split into heavy- (HH) and light- (LH) hole bands as a result of the uniaxial component of the lattice-mismatch strain.

TABLE I. The materials parameters used in calculating the stress-dependent band gaps in $In_xGa_{1-x}As$.

Material	a_l (Å)	a (eV)	b (eV)	C_{11} (10^{11} dyn/cm^2)	C_{12} (10^{11} dyn/cm^2)
GaAs	5.6533[a]	−9.8[b]	−1.76[b]	11.88[a]	5.32[a]
InAs	6.0584[c]	−5.8[b]	−1.8[b]	8.33[c]	4.53[c]

[a]Reference 13.
[b]*Landolt-Börnstein, New Series, Group III*, edited by K. H. Hellwege (Springer-Verlag, Berlin, 1982), Vol. 179.
[c]Reference 16.

from Ref. 16, where m_0 is the free-electron mass. The band alignment was used as an adjustable parameter. Also, since our barriers are relatively thin (≈ 100 Å) coupling effects (miniband dispersion) were taken into account. We have neglected any temperature or stress dependence of the masses in the [001] direction.

IV. EXPERIMENTAL RESULTS

Shown by the dotted lines in Figs. 2 and 3 are the experimental PR spectra at 300 K of samples A and B, respectively. The dotted lines in Figs. 4 and 5 indicate the experimental PR spectra at 77 K from samples A and B, respectively. The solid lines in these figures are a least-squares fit of a line-shape function to the experimental data. In a later section we will discuss in more detail the nature of the line-shape function. The obtained energies of the various transitions are indicated by arrows at the top of the figures. The feature denoted E_0(GaAs) corresponds to the direct band gap of unstrained GaAs and originates in the GaAs buffer-substrate region of the sample. Similar observations have been made in previous PR studies of this system.[4,7] The energy of this feature at 300 and 77 K is used in Eqs. 4(a) and 4(b), respectively, to calculate $E_0(In_xGa_{1-x}As)$.

The energies of the other structures for samples A and B, which originate in the MQW structure, are listed in Tables II and III, respectively. In order to minimize any possible exciton-binding-energy as well as temperature effects we also have listed the energies relative to the lowest-lying feature, which we identify as $11H(\Gamma)$. The notation mnH (or L) indicates transitions from the mth conduction to the nth valence subband of heavy- (H) or light- (L) hole character. The designation Γ (or π) denotes transitions at the minizone center (Γ) or edge (π).

For both samples there is almost no temperature dependence of the intersubband energies relative to $11H(\Gamma)$. This indicates that the major effect of the temperature is to shift the band gaps of the well (and barrier) material. Thus the temperature dependence of the effective masses plays a minor role. The transitions above

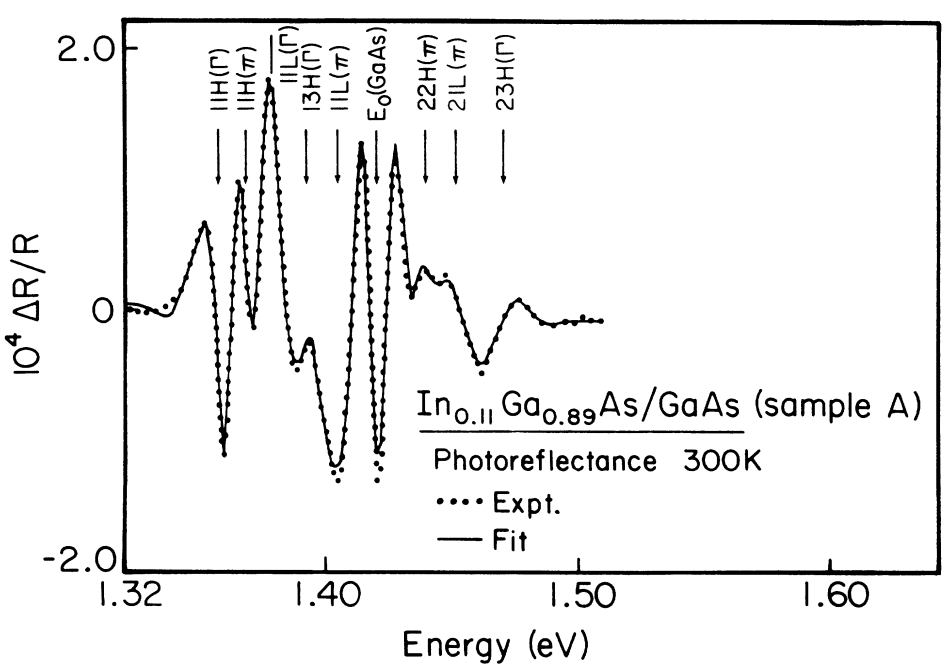

FIG. 2. Photoreflectance spectrum (dotted lines) of an $In_{0.11}Ga_{0.89}As/GaAs$ coupled multiple quantum well (sample A) at 300 K. The solid line is a line-shape fit as discussed in the text.

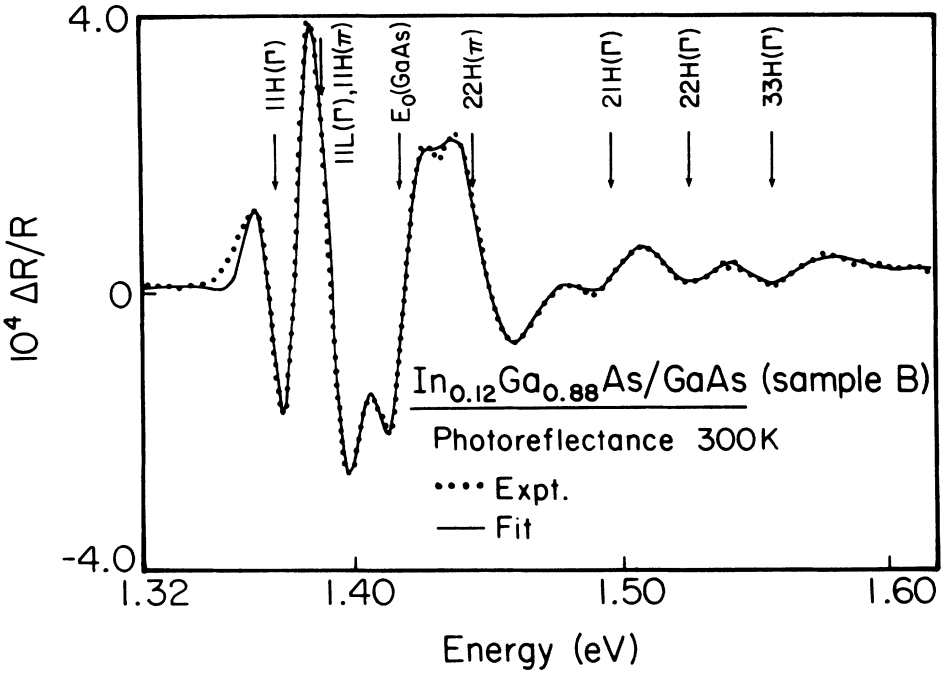

FIG. 3. Photoreflectance spectrum (dotted lines) of an $In_{0.12}Ga_{0.88}As/GaAs$ coupled multiple quantum well (sample B) at 300 K. The solid line is a line-shape fit as discussed in the text.

E_0(GaAs) can clearly be identified as unconfined and occur below the blank lines in Tables II and III.

With regard to the line-shape fit, Shanabrook, Glembocki, and Beard have shown that for uncoupled wells PR yields the first derivative of a Gaussian (or Lorentzian) line-shape function.[17] This is related to the large exciton binding energies in these structures. However, for coupled wells in which tunneling can occur the situation is different since the electron and/or holes can be accelerated by the modulating electric field. This leads to the Aspnes third-derivative functional form[18] for the line shape as demonstrated by a recent experiment comparing PR and thermoreflectance (a first-derivative spectroscopy) line shapes for coupled wells.[19] However, for the

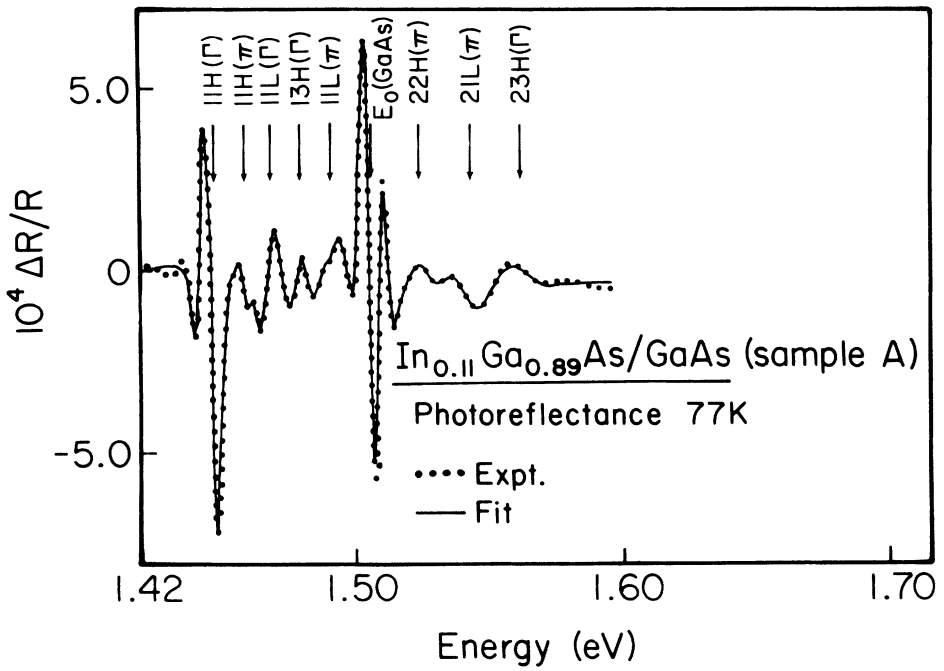

FIG. 4. Photoreflectance spectrum (dotted lines) of an $In_{0.11}Ga_{0.89}As/GaAs$ coupled multiple quantum well (sample A) at 77 K. The solid line is a line-shape fit as discussed in the text.

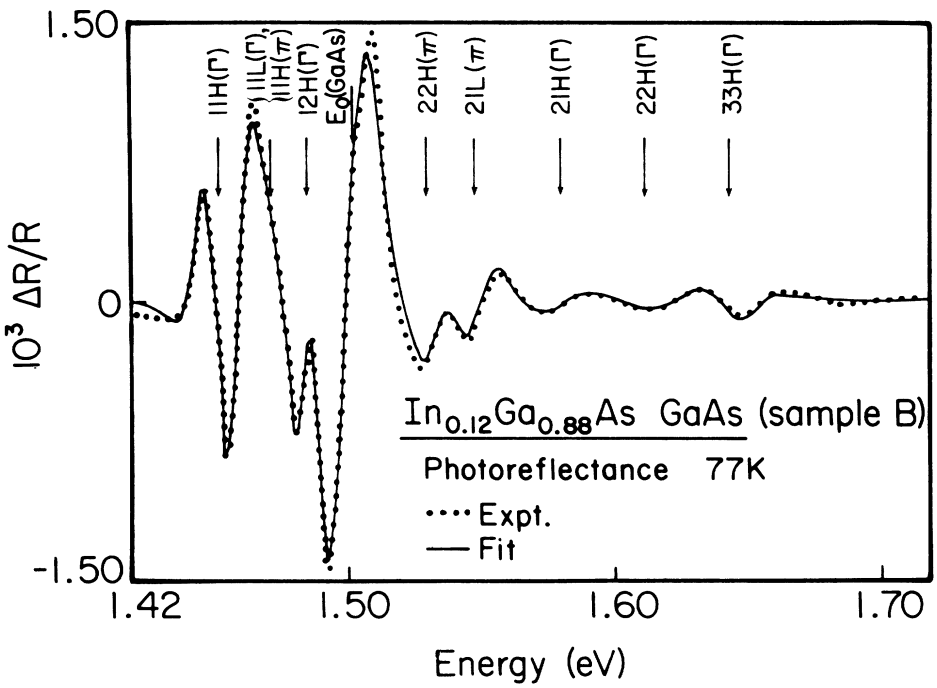

FIG. 5. Photoreflectance spectrum (dotted lines) of an $In_{0.12}Ga_{0.88}As/GaAs$ coupled multiple quantum well (sample B) at 77 K. The solid line is a line-shape fit as discussed in the text.

large number of closely spaced structures observed in our experiment it is not possible to differentiate between various line-shape functions. The fit in Figs. 2–5 is for the third-derivative functional form. A first-derivative functional form yields a comparable fit. The energy positions of the various spectral features are relatively insensitive to the particularly derivative form of the line-shape fit.[17]

V. DISCUSSION OF RESULTS

In order to identify the origins of the various observed PR features we have performed a theoretical calculation based on the envelope-function approach.[9] In addition to energy considerations we have also employed intensity effects (i.e., wave-function overlap) to correlate the spectral features with intersubband transitions. Listed in Tables II and III are the theoretical values of the transition energies for samples A and B, respectively. For the temperature dependence of the various transitions we have taken into account only the temperature dependence of $E_0(In_xGa_{1-x}As)$ and have neglected variations of effective mass with temperature. For sample A the best overall agreement was obtained for $x=0.11\pm0.01$, $L_Z=52\pm3$ Å, $L_B=105\pm5$ Å, and a heavy-hole valence-band offset of 0.30 ± 0.05. For sample B the best fit was found for $x=0.12\pm0.01$, $L_Z=32\pm3$ Å, $L_B=95\pm5$ Å, and a heavy-hole valence-band offset of 0.30 ± 0.05.

Our calculations show that for sample A the strongest

TABLE II. Experimental and theoretical values at 300 and 77 K of the energies of the various features of an $In_{0.11}Ga_{0.89}As/GaAs$ coupled multiple quantum well (sample A). To minimize exciton and temperature effects, the energies relative to the lowest-lying transition, $11H(\Gamma)$, also are listed. The first five features are unconfined. The best theoretical results are obtained for $L_Z=52\pm3$ Å, $L_B=105\pm5$ Å, and a heavy-hole valence-band offset of 0.30 ± 0.05.

Spectral Features	Experiment				Theory			
	300 K		77 K		300 K		77 K	
	E (meV)	$E-E[11H(\Gamma)]$ (meV)	E (meV)	$E-E[11H(\Gamma)]$ (meV)	E (meV)	$E-E[11H(\Gamma)]$ (meV)	E (meV)	$E-E[11H(\Gamma)]$ (meV)
$11H(\Gamma)$	1358±2	0	1448±1	0	1363	0	1453	0
$11H(\pi)$	1368±2	10±4	1459±1	11±2	1371	8	1461	8
$11L(\Gamma)$	1379±3	21±5	1469±2	21±3	1388	25	1478	25
$13H(\Gamma)$	1392±3	34±5	1481±2	33±3	1393	30	1483	30
$11L(\pi)$	1405±5	47±7	1493±4	45±5	1407	44	1497	44
$22H(\pi)$	1439±3	81±5	1527±2	79±3	1438	75	1528	75
$21L(\pi)$	1455±4	97±6	1546±3	98±4	1454	91	1544	91
$23H(\Gamma)$	1476±4	118±6	1565±3	117±4	1490	127	1580	127

TABLE III. Experimental and theoretical values at 300 and 77 K of the energies of the various features of an $In_{0.12}Ga_{0.88}As/GaAs$ coupled multiple quantum well (sample B). To minimize exciton and temperature effects the energies relative to the lowest-lying transition, $11H(\Gamma)$, also are listed. The first four features are unconfined transitions. The best theoretical results are obtained for $L_Z=32\pm3$ Å, $L_B=95\pm5$ Å and a heavy-hole valence-band offset of 0.30 ± 0.05.

Spectral Feature	Experiment				Theory			
	300 K		77 K		300 K		77 K	
	E (meV)	$E-E[11H(\Gamma)]$ (meV)	E (meV)	$E-E[11H(\Gamma)]$ (meV)	E (meV)	$E-E[11H(\Gamma)]$ (meV)	E (meV)	$E-E[11H(\Gamma)]$ (meV)
$11H(\Gamma)$	1372±3	0	1453±2	0	1376	0	1457	0
$11L(\Gamma)$	1389±5	17±8	1473±4	20±6	1397	21	1478	21
$11H(\pi)$					1397	21	1478	21
$12H(\Gamma)$			1487±2	33±4	1409	33	1490	33
$22H(\pi)$	1446±6	74±9	1532±3	79±5	1458	82	1539	82
$21L(\pi)$			1551±3	98±5	1478	102	1559	102
$21H(\Gamma)$	1499±6	127±9	1582±4	129±6	1507	131	1588	131
$22H(\Gamma)$	1528±3	156±6	1616±5	163±7	1540	164	1621	164
$33H(\Gamma)$	1560±6	188±9	1646±4	193±6	1566	190	1647	190

below-barrier features are the "symmetry-allowed" transition $11H(\Gamma)$, $11H(\pi)$, and $11L(\Gamma)$, all of comparable magnitude. The "symmetry-forbidden" transition $13H(\Gamma)$ as well as $11L(\pi)$ should be quite weak. The above-barrier transitions $22H(\pi)$, $21L(\pi)$, and $23H(L)$ have the strongest overlap matrix elements in this energy range. For sample B all the features except $12H(\Gamma)$ (observed at 77 K only) and $21H(\Gamma)$ have strong overlap matrix elements.

The symmetry properties of transitions whose energy is near or above the barrier are more complicated in relation to deeply confined features. The wave functions of deeply confined states do not penetrate into the barrier, i.e., there is a node at the well/barrier interface. Thus the selection rule $m=n$ is applicable because of the relatively simple relationship between the number of nodes of the wave function in the well and the energy of that state. However, for the former states there may be considerable penetration of the wave function into the barrier region. Additional nodes may appear in the barrier and hence the parities of the states (with respect to the center of the well) do not alternate. As a consequence, these states no longer make a ladder in energy with respect to the previous one.[20–22] Therefore, in order to identify the strongest near- and above-barrier transitions a detailed calculation of matrix elements (overlap integrals) must be performed. Both the tight-binding and envelope-function models have proven to be valid for such evaluations.[20–22]

In general, there is very good agreement between the experimentally observed energies and our envelope-function calculation, as can be seen in Tables II and III. For the $11H(\Gamma)$ transition there is about a 4–5 meV difference, which may be due to exciton effects. For uncoupled states the exciton binding energy should be about 10 meV for $In_xGa_{1-x}As$ ($x\approx0.12$) with such narrow wells.[9,23] However, the coupling probably reduces this value. Therefore 4–5 meV is quite reasonable for the exciton binding energy in such strongly coupled states. Note, that for the energies relative to $11H(\Gamma)$ there is excellent agreement between theory and experiment.

For sample B the strongest below-barrier feature at both 300 and 77 K is $11L(\Gamma), 11H(\pi)$, i.e., there is an accidental degeneracy of these two transitions. For sample A, because of the larger L_Z, the transition $11H(\pi)$ lies below $11L(\Gamma)$ and they are clearly resolved at both temperatures. This degeneracy in sample B is an important clue to the band offset. Plotted in Fig. 6 are the energies of $11H(\Gamma)$, $11H(\pi)$, and $11L(\Gamma)$ as a function of conduction-band offset, Q_C, for the physical parameters of sample B ($x=0.12\pm0.01$, $L_Z=32\pm3$ Å, and $L_B=95\pm5$ Å). Note that for $Q_C\approx0.7$ the transitions $11H(\pi)$ and $11L(\Gamma)$ are degenerate. Thus $Q_V^{HH}=0.3$ for this value of Q_C.

We now turn our attention to the $11L(\pi)$ transitions. It can be demonstrated, from both symmetry arguments as well as a detailed matrix-element (wave-function overlap) calculation, that if the light holes are confined in the GaAs region, $11L(\pi)$ should be a very weak feature.

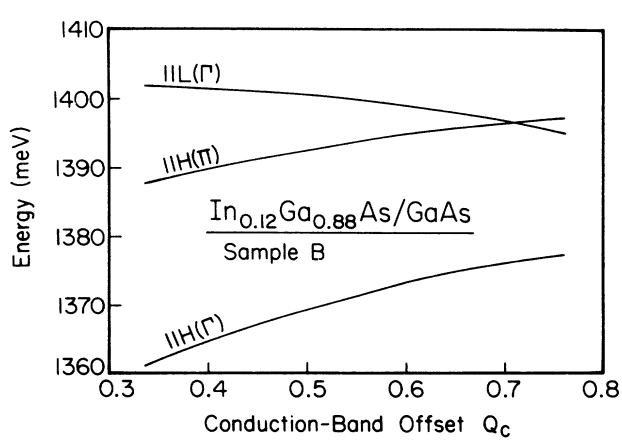

FIG. 6. Theoretical values of the energies of $11H(\Gamma)$, $11H(\pi)$, and $11L(\Gamma)$ for an $In_{0.12}Ga_{0.88}As/GaAs$ coupled multipole quantum well (sample B) as a function of conduction-band–offset parameter, Q_C ($=1-Q_V$).

This transition corresponds to the antisymmetric component of the splitting caused by the coupling, while $11L(\Gamma)$ is related to the symmetric component. It can also be shown that even for a type-II configuration $11L(\Gamma)$ is still fairly strong. These considerations are certainly consistent with our observation for sample B, in which we do not observe $11L(\pi)$, which should occur about 60 meV above $11H(\Gamma)$. Note that there is no feature in this energy range in Fig. 3 or 5. For sample A we apparently do observe $11L(\pi)$, but it is difficult to determine its amplitude since it occurs on the low-energy side of E_0(GaAs). It has been demonstrated that there are often considerable interference effects on the low-energy shoulders of features originating from the barrier and/or substrate.[19,24] This complicates the evaluation of the amplitude of $11L(\pi)$ for sample A. However, the situation of sample B is clear. The fact that we can clearly observe $11L(\Gamma)$ for sample A demonstrates that "spatially indirect" transitions can be observed in modulated reflectivity, as first pointed out in Refs. 4 and 7.

We now turn our attention to the question of the band lineups at the $In_xGa_{1-x}As$/GaAs heterojunction. For strained-layer systems a convenient quantity is the average valence-band edge E_V^{av} given by

$$E_V^{av}=\tfrac{1}{3}(E_V^{HH}+E_V^{LH}+E_V^{SO}) , \tag{6a}$$

where E_V^{SO} is the spin-orbit-split valence band. The parameter E_V^{av} is useful because it is independent of the uniaxial component of the strain. Thus, we can define

$$\Delta E_V^{av}=E_V^{av}(In_xGa_{1-x}As)-E_V^{av}(GaAs) . \tag{6b}$$

Based on our result of $Q_V^{HH}=0.3\pm0.05$ for samples with $x\approx0.12$, we find that a linear extrapolation to $x=1$ yields $\Delta E_V^{av}=0.1\pm0.1$ eV for the InAs/GaAs interface. Menendez *et al.* report $\Delta E_V^{av}=0.49\pm0.10$ eV extrapolated to the InAs-GaAs system.[18] A similar value for the band lineup also has been deduced from measurements on $In_xGa_{1-x}As$/GaAs bipolar structures.[25] There have been several theoretical calculations of the band lineup of this system. Using a self-consistent calculation, including strain effects, Van de Walle finds $\Delta E_V^{av}=0.37$ for the [001] InAs/GaAs interface.[26] Using midgap theories Tersoff[27] obtains 0.0 eV, while Cardona and Christensen[28] find $\Delta E_V^{av}=-0.15$ eV. These values should be corrected for the hydrostatic-pressure component of the strain. However, this effect should be quite small.[28] As pointed out in Ref. 26 the above value is based on a preliminary calculation for the [001] interface. The author notes that a full study should really include a determination of the stable structure by minimization of the total energy with respect to the atomic positions near the interface. Van de Walle has assumed that the InAs and GaAs bond lengths at the interface are equal and given by the average of the bond lengths in each material (one of which is strained). It turns out that the band lineups are fairly sensitive to the choice of this parameter; changing the position of the As atom by 0.1 Å in the [001] direction can shift the lineups by as much as 0.3 eV.

Thus, the question of the band lineup in this system has not yet been resolved, either experimentally or theoretically. Based on Van de Walle's result concerning the sensitivity of ΔE_V^{av} to the position of the As atom, it may be that samples grown under slightly different growth conditions could have different ΔE_V^{av}. Certainly more work needs to be done, particularly if several different experiments (PR, light scattering, electrical) could be done on the same sample.

VI. SUMMARY

We have performed PR on two [001] $In_xGa_{1-x}As$/GaAs strained-layer, coupled MQW's. We have observed a number of features corresponding to miniband dispersion of both confined and unconfined states. Comparison of the experimental intersubband energies with an envelope-function calculation yields $x=0.11\pm0.01$, $L_Z=52\pm3$ Å, and $L_B=105\pm5$ Å for sample A and $x=0.12\pm0.01$, $L_Z=32\pm3$ Å, and $L_B=95\pm5$ Å for sample B. These physical parameters are in good agreement with those deduced from the growth conditions. For both samples we find a heavy-hole valence-band–offset parameter of 0.3 ± 0.05. This value is consistent with several other optical studies, but is in disagreement with a recent evaluation using a light-scattering technique. Comparison between our experimental value and several theoretical calculations has been made.

ACKNOWLEDGMENTS

Four of the authors (S.H.P., H.S., Z.H., and F.H.P.) acknowledge the support of Professional Staff Congress of the City University of New York (PSC/CUNY) Grant No. RF-6-67350 and the New York State Foundation for Science and Technology as a part of its Center for Advanced Technology Program. We have benefited from a number of conversations with C. G. Van de Walle, A. Pinzcuk, and J. Menendez. The support of the National Science Foundation of China is acknowledged by one of us (W.Z.). We wish to thank Y. Tang for valuable assistance.

*Permanent address: Department of Physics, Nankai University, Tianjin, Hefei, China.

†Also at Graduate School and University Center of the City University of New York, New York, NY 10036.

[1]J.-Y. Marzin, M. N. Charasse, and B. Sermage, Phys. Rev. B **31**, 8298 (1985).

[2]A. P. Roth, R. A. Masut, M. Sacilotti, P. J. D'Arcy, Y. Le Page, G. I. Sproule, and D. F. Mitchell, Superlattices Microstruct. **2**, 507 (1986).

[3]N. G. Anderson, W. D. Laidig, R. M. Kolbas, and Y. C. Lo, J. Appl. Phys. **60**, 2361 (1986).

[4]U. K. Reddy, G. Ji, R. Houdre, H. Unlu, D. Huang, and H.

Morkoç, Proc. Soc. Photo-Opt. Instrum. Eng. **794**, 116 (1987).

[5]G. Ji, D. Huang, U. K. Reddy, H. Unlu, T. S. Henderson, and H. Morkoç, J. Vac. Sci. Technol. B **5**, 1346 (1987).

[6]G. Ji, D. Huang, U. K. Reddy, T. S. Henderson, R. Houdre, and H. Morkoç, J. Appl. Phys. **62**, 3366 (1987).

[7]G. Ji, U. K. Reddy, D. Huang, T. S. Henderson, and H. Morkoç, Superlattices Microstruct. (to be published).

[8]J. Menendez, A. Pinczuk, D. J. Werder, S. K. Sputz, R. C. Miller, D. L. Sivco, and A. Y. Cho, Phys. Rev. B **36**, 8165 (1987).

[9]G. Bastard and J. A. Brum, IEEE J. Quant. Electron **QE-22**, 1625 (1986).

[10]A. P. Roth, M. A. Sacilotti, R. A. Masut, A. Machado, and J. P. D'Arcy, J. Appl. Phys. **60**, 2003 (1986).

[11]H. Shen, P. Parayanthal, Y. F. Liu, and F. H. Pollak, Rev. Sci. Instrum. **58**, 1429 (1987).

[12]F. H. Pollak, Surf. Sci. **37**, 863 (1973).

[13]S. Adachi, J. Appl. Phys. **58**, R1 (1985).

[14]Y. L. Leu, F. A. Thiel, H. Scheiber, B. I. Miller, and J. Backmann, J. Electron. Mater. **8**, 663 (1979).

[15]O. Berolo and J. C. Wooley, in *Proceedings of the 11th International Conference on the Physics of Semiconductors, Warsaw, 1972* (Polish Scientific, Warsaw, 1972), p. 1420.

[16]S. Adachi, J. Appl. Phys. **53**, 8775 (1982).

[17]B. V. Shanabrook, O. J. Glembocki, and W. T. Beard, Phys. Rev. B **35**, 2540 (1987).

[18]D. E. Aspnes, in *Handbook on Semiconductors,* edited by T. S. Moss (North-Holland, New York, 1980), Vol. 2, p. 109; H. Shen, P. Parayanthal, F. H. Pollak, M. Tomkiewicz, T. J. Drummond, and J. N. Schulman, Appl. Phys. Lett. **48**, 653 (1986).

[19]H. Shen, S. H. Pan, F. H. Pollak, and R. N. Sacks, Phys. Rev. B **37**, 10 919 (1988).

[20]J. J. Song, Y. S. Yoon, P. S. Jung, A. Fedotowsky, J. N. Schulman, C. W. Tu, J. M. Brown, D. Huang, and H. Morkoç, Appl. Phys. Lett. **50**, 1269 (1987).

[21]U. K. Reddy, G. Ji, T. Henderson, H. Morkoç, and J. N. Schulman, J. Appl. Phys. **62**, 145 (1987).

[22]H. Shen, S. H. Pan, Z. Hang, F. H. Pollak, and R. N. Sacks, Solid State Commun. **65**, 929 (1988).

[23]K. K. Bajaj (private communication).

[24]X. L. Zhang, D. Heiman, B. Lax, and F. H. Chambers, Appl. Phys. Lett. **52**, 287 (1988).

[25]L. P. Ramberg, P. M. Enquist, Y. K. Chen, F. E. Najjar, L. F. Eastman, E. A. Fitzgerald, and K. L. Kavanagh, J. Appl. Phys. **61**, 1234 (1987).

[26]C. G. Van de Walle, Ph.D. thesis, Standford University, 1986 (unpublished).

[27]J. Tersoff, Phys. Rev. Lett. **56**, 2755 (1986).

[28]M. Cardona and N. E. Christensen, Phys. Rev. B **35**, 6182 (1987).